Polyelectrolyte adsorption: Chemical and electrostatic interactions

Adi Shafir* and David Andelman†
School of Physics and Astronomy, Raymond and Beverly Sackler Faculty of Exact Sciences, Tel Aviv University, Ramat Aviv, Tel Aviv 69978, Israel

(Received 3 December 2003; revised manuscript received 24 August 2004; published 28 December 2004)

Mean-field theory is used to model polyelectrolyte adsorption and the possibility of overcompensation of charged surfaces. For charged surfaces that are also chemically attractive, the overcharging is large in high salt conditions, amounting to 20–40 % of the bare surface charge. However, full charge inversion is not obtained in thermodynamical equilibrium for physical values of the parameters. The overcharging increases with addition of salt, but does not have a simple scaling form with the bare surface charge. Our results indicate that a more evolved explanation is needed in order to understand polyelectrolyte multilayer buildup. For strong polymer-repulsive surfaces, we derive simple scaling laws for the polyelectrolyte adsorption and overcharging. We show that the overcharging scales linearly with the bare surface charge, but its magnitude is very small in comparison to the surface charge. In contrast with the attractive surface, here the overcharging is found to decrease substantially with addition of salt. In the intermediate range of weak repulsive surfaces, the behavior with addition of salt crosses over from increasing overcharging (at low ionic strength) to a decreasing one (at high ionic strength). Our results for all types of surfaces are supported by full numerical solutions of the mean-field equations.

DOI: 10.1103/PhysRevE.70.061804 PACS number(s): 82.35.Gh, 82.35.Rs, 61.41.+e

I. INTRODUCTION

Aqueous solutions containing polyelectrolytes and small ions are abundant in biological systems, and have been the subject of extensive research in recent years. When such a solution is in contact with an oppositely charged surface, adsorption of the polyelectrolyte chains can occur. Theoretical descriptions of polyelectrolyte adsorption take into account the multitude of different interactions and length scales. Among others they include electrostatic interactions between the surface, monomers, and salt ions, excluded-volume interactions between monomers and entropy considerations. Although a full description of polyelectrolytes is still lacking at present, several approaches exist and use different types of approximations [1–23]. These include linearized mean-field equations [1–6], numerical solutions of nonlinear mean-field equations [7–10], scaling considerations [7–16], multi-Stern layers of discrete lattice models [17–20], and computer simulations [21–23].

Experimental studies [24–26] have shown that adsorbing polyelectrolytes (PE's) may carry a charge greater than that of the bare surface, so that the overall surface-polyelectrolyte complex has a charge opposite to that of the bare charged surface. This phenomenon is known as *overcharging* (or surface charge *overcompensation*) by the PE chains. When the overcharging is large enough to completely reverse the bare surface charge, the resulting charge surplus of the complex can be used to attract a second type of polyelectrolyte having an opposite charge to that of the first polyelectrolyte layer. Eventually, by repeating this process, a complex structure of alternating layers of positively and negatively charged polyelectrolytes can be formed. Experimentally, multilayers consisting of hundreds of such layers can be created [24,25], leading the way to several interesting applications.

A theoretical description of the PE overcharging was proposed in Refs. [6,27,28] based on a mean-field formalism. The model relies on several approximations for a very dilute PE solution in contact with a charged surface and in theta solvent condition. In the high salt limit, the model predicts an exact charge inversion for *indifferent* (i.e., noninteracting) surfaces. In another work [7], the scaling of the adsorption parameters was derived using a Flory-like free energy. This work used mean-field theory, but with a different type of boundary conditions. Using a strongly (nonelectrostatic) repulsive surface for the PE, profiles of monomer concentration and electrostatic potential have been calculated from numerical solution of the mean-field equations. Several scaling laws have been proposed and the possibility of a weak overcharging in low salt condition has been demonstrated. In a related work [10] we presented simple scaling laws resulting from the same mean-field equations and for the same chemically repulsive surfaces. In particular, we addressed the adsorption-depletion crossover as function of added salt. We showed that addition of salt eventually causes the polyelectrolyte to deplete from the charged surface, and pre-empts the high-salt adsorption regime described in Ref. [7].

The present paper can be regarded as a sequel to Ref. [10], offering a more complete treatment of the adsorption problem for several types of charged surfaces. In particular, it includes the effect of surface-PE chemical interactions, and the scaling of overcharging and adsorption in the presence of added salt. These chemical interactions are found to play a crucial role in the overcharging, showing that a necessary condition for the formation of multilayers is a chemical attraction of nonelectrostatic origin (complexation) between the two types of PE chains as well as between the PE and the charged surface. For chemically attractive surfaces our re-

*Electronic address: shafira@post.tau.ac.il
†Electronic address: andelman@post.tau.ac.il

sults deviate from those of Refs. [6,27,28]. We find in the same solvent and surface conditions that the overcharging does not reach a full 100% charge inversion of the bare surface charge. It rather depends on system parameters and never exceeds 30–40 % for the physical range of parameters. Like in Ref. [6], we find an increase of the overcharging with salt but our numerical results do not agree with the previous prediction. For repulsive surfaces, several scaling laws are obtained and agree well with the numerically obtained profiles. However, due to the competition between the electrostatic and chemical surface interactions, the overcharging here is usually quite small, of the order of $\sim 1\%$ only.

The paper is organized as follows: the mean-field equations, used in the past in several other works for PE adsorption, are reviewed in Sec. II. The following two sections treat two different types of surfaces. In Sec. III, results for PE adsorption and overcharging for attractive surfaces are presented and compared with previous models. In Sec. IV we derive the scaling of adsorbed PE layers in the case of a chemically repulsive surface. In Sec. V we present the adsorption and overcharging for the intermediate case of a weakly repulsive surface. In particular, we show the dependence of PE adsorption on the solution ionic strength. A summary of the main results and future prospects are presented in Sec. VI.

II. MEAN-FIELD EQUATIONS AND SURFACE CHARACTERISTICS

Consider an aqueous solution, containing a bulk concentration of infinitely long polyelectrolyte (PE) chains, together with their counterions and a bulk concentration of salt ions. Throughout this paper we assume for simplicity that the PE's are positively charged and that the counterions and added salt are all monovalent. The mean-field equations describing such an ionic solution have been derived elsewhere [7,10] and are briefly reviewed here:

$$\nabla^2\psi = \frac{8\pi e c_{\rm salt}}{\epsilon}\sinh(\beta e\psi) + \frac{4\pi e}{\varepsilon}(\phi_b^2 f e^{\beta e\psi} - f\phi^2), \quad (1)$$

$$\frac{a^2}{6}\nabla^2\phi = v(\phi^3 - \phi_b^2\phi) + \beta f e\psi\phi, \quad (2)$$

where the polymer order parameter $\phi(\mathbf{r})$ is the square root of $c(\mathbf{r})$, the local monomer concentration, ϕ_b^2 the bulk monomer concentration, ψ the local electrostatic potential, $c_{\rm salt}$ the bulk salt concentration, ε the dielectric constant of the aqueous solution, f the monomer charged fraction, e the electron charge, v the second virial (excluded volume) coefficient of the monomers, a the monomer size, and $\beta = 1/k_BT$ the inverse of the thermal energy. Equation (1) is the Poisson-Boltzmann equation where the salt ions, counterions, and monomers are regarded as sources of the electrostatic potential. Equation (2) is the mean-field (Edwards) equation for the polymer order parameter $\phi(\mathbf{r})$, where the excluded-volume interaction between monomers and external electrostatic potential $\psi(\mathbf{r})$ are taken into account.

For the case of an infinite planar wall at $x=0$, Eqs. (1) and (2) can be transformed into two coupled ordinary differential equations, which depend only on the distance x from the surface,

$$\frac{d^2\zeta}{dx^2} = \kappa^2\sinh\zeta + k_m^2(e^{\zeta} - \eta^2), \quad (3)$$

$$\frac{a^2}{6}\frac{d^2\eta}{dx^2} = v\phi_b^2(\eta^3 - \eta) + f\zeta\eta, \quad (4)$$

where $\zeta \equiv e\psi/k_BT$ is the dimensionless (rescaled) electrostatic potential, $\eta^2 \equiv \phi^2/\phi_b^2$ the dimensionless monomer concentration, $\kappa^{-1} = (8\pi l_B c_{\rm salt})^{-1/2}$ the Debye-Hückel screening length, due to added salt concentration, $k_m^{-1} = (4\pi l_B \phi_b^2 f)^{-1/2}$ a similar decay length due to counterions, and $l_B = e^2/\varepsilon k_BT$ the Bjerrum length. For water with dielectric constant $\varepsilon = 80$ at room temperature, l_B is equal to about 7 Å. Note that the actual decay of the electrostatic potential is determined by a combination of salt, counterions, and polymer screening effects.

The solution of Eqs. (3) and (4) requires four boundary conditions for the two profiles. The electrostatic potential decays to zero at infinity, $\zeta(x\to\infty)=0$. At the surface, we have chosen to work with a constant surface potential. Namely, a conducting surface with a potential $\psi=\psi_s$, or in rescaled variables, $\zeta(0) = -|\zeta_s|$. The results can be easily extended to the case of fixed surface charge density (which amounts to fixing the derivative of the potential $d\zeta/dx|_{x=0} = -4\pi l_B\sigma$).

For the PE profile we also have two boundary conditions. At infinity, $\eta(x\to\infty)=1$, because $\phi(\infty)=\phi_b$ has to match the bulk value. The special case of a zero bulk monomer concentration can be treated by taking $\phi_b \to 0$ and working directly with the nonrescaled concentration $\phi(x)$.

We model separately two types of surfaces. Although the surface always attracts the oppositely charged PE chains, it can be either chemically repulsive or attractive. In the case of a chemical repulsion between the PE chains and the surface, the amount of PE chains in direct contact with the surface is set to a small value $\eta(x=0)=\eta_s$. In the limit of a strong repulsive surface, η_s tends to zero and the boundary condition is $\eta(x=0)=0$. Because of the ever-present longer-range electrostatic attraction with the surface, PE chains accumulate in the surface vicinity, resulting in a positive slope $d\eta/dx|_{x=0} > 0$.

For chemical attractive surfaces we rely on a boundary condition often used [6,29] for neutral polymer chains: $d\eta(0)/dx + \eta(0)\cdot d^{-1} = 0$ where d has units of length and is inversely proportional to the strength of nonelectrostatic interactions of the PE's with the surface. The limit of $d\to\infty$ is the *indifferent* (noninteracting) surface limit, while the previous limit of a strong repulsive surface is obtained by a small and negative d.

In the following sections we present our results, first for the chemically attractive surface and then for the chemically repulsive one.

III. OVERCHARGING OF CHEMICALLY ATTRACTIVE SURFACES

In this section we restrict the attention to surfaces that attract the polymer in a nonelectrostatic (short range) fashion. For example, a possible realization can be a system containing PE chains with hydrophobic groups (like polystyrene sulfonate) that are attracted to a hydrophobic surface, like the water-air interface. The short range attraction is modeled by a surface interaction in a similar way that is used extensively for neutral polymers via a boundary condition on the polymer order parameter at the surface $x=0$:

$$\eta(0) = -d \cdot \left.\frac{d\eta}{dx}\right|_{x=0}, \tag{5}$$

where the length d was introduced in Sec. II and is inversely proportional to the strength of the surface interaction.

Close to a surface the polymer has a concentration profile given in terms of the distance from the surface x. Within mean-field theory the adsorbed polymer amount is defined with respect to the bulk concentration ϕ_b^2 to be

$$\Gamma \equiv \int_0^\infty dx(\phi^2 - \phi_b^2) = \phi_b^2 \int_0^\infty dx(\eta^2 - 1). \tag{6}$$

We note that the definition of Γ manifests one of the deficiencies of mean-field theory where it is not possible to distinguish between chains absorbed on the surface and those accumulated in the surface vicinity. The latter will be washed away when the surface is placed in a clean aqueous solution and does not participate in the effective PE surface buildup.

Another important quantity to be used throughout this paper is the overcharging parameter defined as the excess of PE charge over that of the bare surface charge per unit area, σ:

$$\Delta\sigma \equiv -|\sigma| + f\Gamma, \tag{7}$$

where $\sigma<0$ is the *induced* surface charge density calculated from the fixed surface potential ($\zeta' = -4\pi l_B \sigma$) in units of e, the electron charge. Note that in terms of the relative overcharging parameter $\Delta\sigma/|\sigma|$, $-1 \leqslant \Delta\sigma/|\sigma| \leqslant 0$ corresponds to *undercharging*, while a positive $\Delta\sigma/|\sigma| > 0$ to overcharging. The special value $\Delta\sigma/|\sigma| = 1$ indicates a *full* charge inversion.

We solved numerically the mean-field coupled equations, Eqs. (3) and (4), with the electrostatic boundary condition of a fixed surface potential $|\zeta_s|$ (that has a one-to-one correspondence with an induced surface charge density σ) and a nonelectrostatic boundary condition from Eq. (5). The relative overcharging $\Delta\sigma/|\sigma|$ is plotted in Fig. 1 as function of the amount of salt. The solid line represents our numerical results, while the dashed one corresponds to a previous prediction [6]. The same system parameters are used for both: the limit of a dilute PE reservoir ($\phi_b=0$), theta solvent conditions ($v=0$), a strong ionic strength, and an indifferent surface taken in the limit of $d\to\infty$ (obtained already for $d \geqslant 100$ Å). Figure 1 shows an increasing dependence of the overcharging parameter on c_{salt}, but does not obey any simple scaling law. It varies on quite a large range of values from less than 10% (relative to $|\sigma|$) for $c_{\text{salt}} \simeq 0.1M$ to about

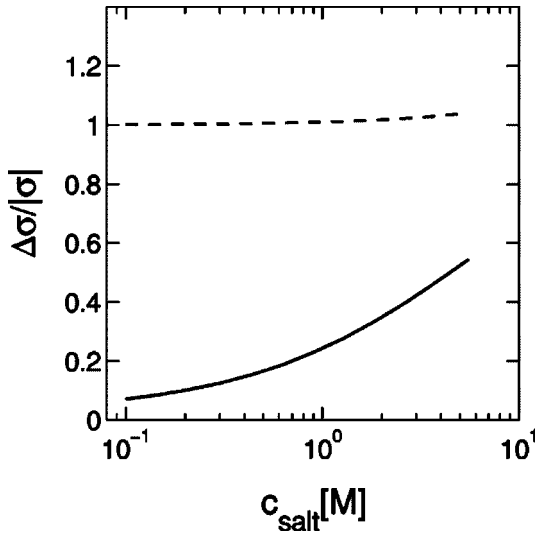

FIG. 1. The relative overcharging, $\Delta\sigma/|\sigma| = (f\Gamma - |\sigma|)/|\sigma|$, is presented as a function of the amount of added salt c_{salt}. The solid line corresponds to the numerical results (Sec. III), while the dashed line corresponds to the predictions from Eq. (9) in Ref. [6]. As the surface potential $|\zeta_s|$ is fixed, σ is the numerically calculated induced surface charge. The numerical results show a much lower overcharging than the predicted ones. Furthermore, the salt dependence of the overcharging is shown to be much stronger. The system parameters have been chosen to match those of Ref. [6]. A dilute aqueous solution ($\phi_b=0$), in theta solvent conditions ($v=0$) is used. Other parameters are $\varepsilon=80$, $T=300$ K, $|\zeta_s|=1.0$, $a=5$ Å, $f=1$, $d=100$ Å.

55% for $c_{\text{salt}} \simeq 5.5M$. We never observed for reasonable values of the parameters a full charge inversion of 100% or more.

Our results are contrasted with the approximated prediction of Ref. [6]. In the high salt limit the prediction reads

$$\frac{\Delta\sigma}{|\sigma|} = 1 + \frac{2a^2}{3df|\sigma|} c_{\text{salt}}, \tag{8}$$

where we note that in Ref. [6] all lengths are rescaled with $a/\sqrt{6}$. This prediction is shown by the dashed line in Fig. 1. One can see that the linear dependence on salt concentration is very weak and that for the entire range of salt the result is dominated by the first and constant term in Eq. (8), giving an overcharging of 100–110 %. Although the general trend of an increase in $\Delta\sigma/|\sigma|$ appears in both results, there is neither agreement in the values of $\Delta\sigma/|\sigma|$ nor in the quantitative dependence on c_{salt} for a wide range of c_{salt} values.

The results of Fig. 1 have been done in the limit of an indifferent surface modeled by $d \gg \kappa^{-1}$. A closer examination of the overcharging d dependence is presented in Fig. 2. Both in part (a) for $f=0.2$ and in part (b) for $f=1$, our result and the prediction of Eq. (8) show a similar descending trend with d. Already for d as small as 100 Å the asymptotic results for the indifferent surface result is obtained. For smaller d, the chemical attraction causes a bigger overcharging. The main discrepancy between our exact solution of the mean-field equations and Eq. (8) is in the actual limiting value for $d\to\infty$ and the lack of charge inversion from our results

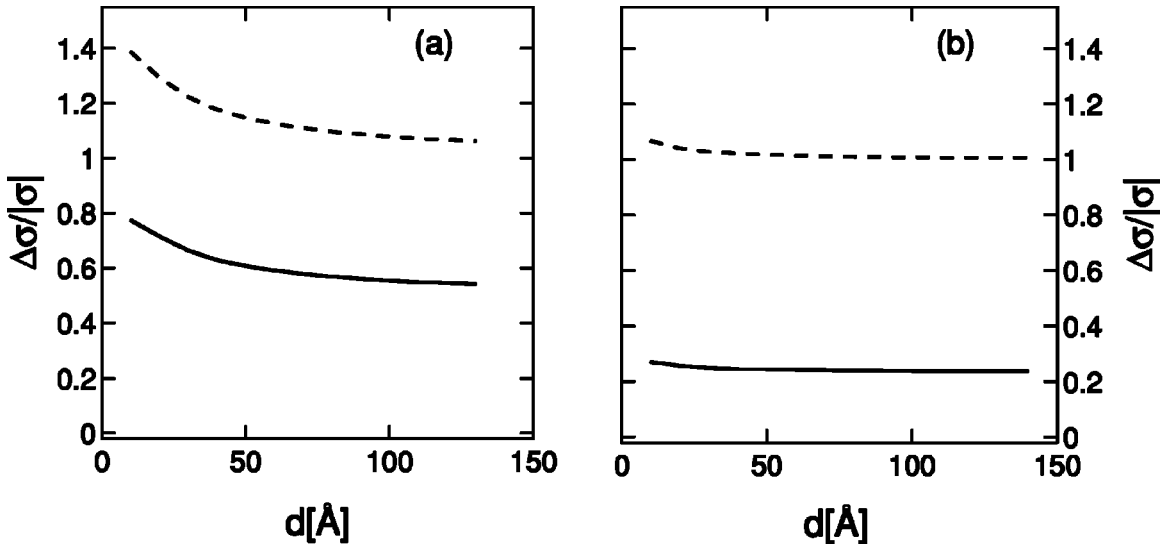

FIG. 2. The relative overcharging, $\Delta\sigma/|\sigma|$, is plotted against the chemical interaction parameter d, for (a) $f=0.2$ and (b) $f=1$. The solid line corresponds to the numerically calculated relative overcharging, while the dashed line corresponds to the theoretical predictions taken from Ref. [6]. Unlike the previous prediction, we do not observe a full charge inversion. The calculations are done in high salt conditions $c_{\text{salt}}=1M$, corresponding to a Debye length of about 3 Å. Other parameters used are the same as in Fig. 1. Although the numerical and predicted profiles show a similar qualitative dependence with d, they do not coincide, and converge to different values at $d\to\infty$. For practical purposes, $d=100$ Å is already a very good approximation for the indifferent $d\to\infty$ surface.

(solid line in Fig. 2). Note also that the difference between the two results cannot be explained by a constant multiplicative factor, and that $\Delta\sigma/|\sigma|$ is smaller for $f=1$ than for $f=0.2$ due to the larger electrostatic repulsion between charged monomers.

To complete the presentation of the attractive surface we show in Fig. 3 the dependence of the overcharging on c_{salt} for several different values of surface potential, ranging from $|\zeta_s|=1$ to 0.2. In part (a) the PE absorbed amount Γ (in units of Å^{-2}) is shown while in part (b) the dimensionless $\Delta\sigma/|\sigma|$ is shown. The general trend is an increase of both quantities with c_{salt} due to the nonelectrostatic attraction of the PE chain to the surface on one hand and the screening of the monomer-monomer repulsion on the other. The overcharging

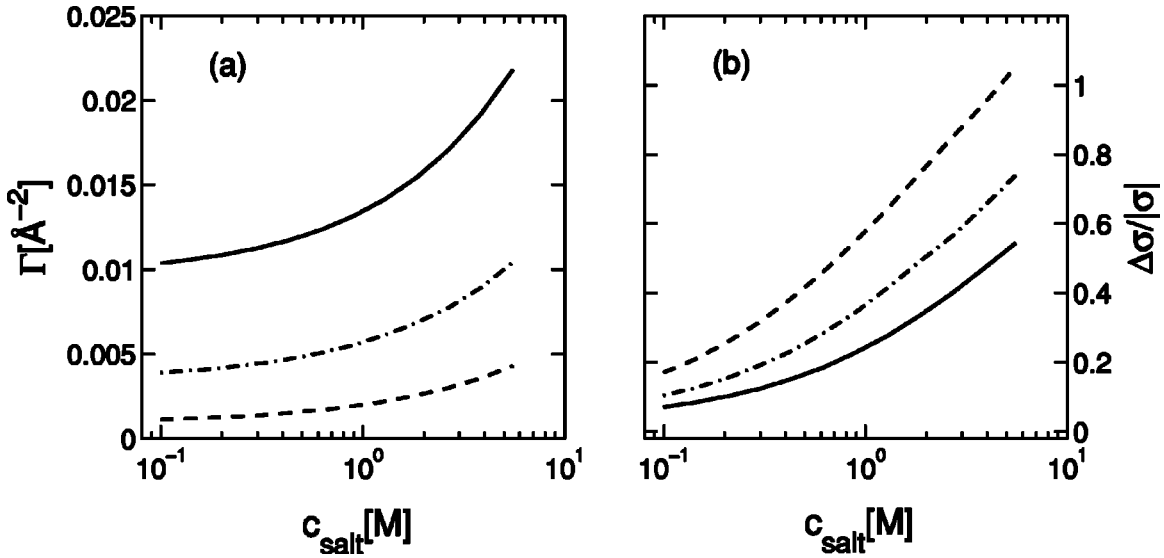

FIG. 3. (a) The numerically calculated adsorbed amount $\Gamma=\int_0^\infty dx(\phi^2-\phi_b^2)$ is plotted as a function of the amount of added salt for three values of the surface potential $|\zeta_s|$. The solid line corresponds to $|\zeta_s|=1.0$, the dashed-dotted line to $|\zeta_s|=0.5$, and the dashed line to $|\zeta_s|=0.2$. The adsorbed amount is shown to increase both with the amount of added salt and with $|\zeta_s|$. Other parameters used are as in Fig. 1. In (b) the same results are plotted for $\Delta\sigma/|\sigma|$ as a function of the amount of added salt. The relative overcharging $\Delta\sigma/|\sigma|$ is seen to decrease with $|\zeta_s|$, in contrast to Γ where it increases [see part (a)]. This implies that the surface charge σ has a stronger dependence on $|\zeta_s|$ than the adsorbed amount Γ. Therefore, the adsorbed amount no longer scales with σ for attractive surfaces, in contrast to repulsive surfaces, Eq. (18).

is less than 100% unless the amount of salt is unrealistically large. Another observation can be seen from the behavior of $\Delta\sigma/|\sigma|$. We clearly see that $\Delta\sigma$ does not depend linearly on σ since the three different $|\zeta_s|$ give three different curves (no data collapse).

This very last result should be compared with the chemically repulsive surfaces which is discussed next and for which we find that $\Delta\sigma \sim \sigma$.

IV. STRONG CHEMICALLY REPULSIVE SURFACES

The chemical repulsion between the PE chains and the surface causes the amount of PE chains in direct contact with the surface to diminish or even be zero for the strong repulsive case. The latter limit is incorporated into the mean-field equations by taking the boundary condition $\eta_s=0$, used previously in Refs. [7,10].

Our assumptions for treating the adsorbed layer are as follows. (i) Inside the adsorption layer, the electrostatic interactions are assumed to be stronger than the excluded-volume interactions. (ii) Using results from Ref. [10], we assume that the electrostatic potential decays mainly via the PE adsorption and not via the salt (for weak enough ionic strength). (iii) Another assumption is that the electrostatic potential $\zeta \equiv e\psi/k_BT$ can be written in terms of a scaling function $\zeta=|\zeta_s|h(x/D)$, where $|\zeta_s|$ is the surface potential and D is the adsorption layer length scale (see also Ref. [10]). (iv) The last assumption is that the electrostatic potential ζ is low enough so that we can employ the linear Debye-Hückel approximation.

A. First integration of the mean-field equations

The salt dependence of the adsorption characteristic can be obtained from the first integration of Eqs. (3) and (4). Multiplying Eq. (3) by $d\zeta/dx$ and Eq. (4) by $d\eta/dx$, and then integrating both equations from x to infinity yields

$$\frac{1}{2}\left(\frac{d\zeta}{dx}\right)^2 = \kappa^2(\cosh\zeta - 1) + k_m^2\left(e^{\zeta} - 1 + \int_x^{\infty} \eta^2 \frac{d\zeta}{dx} dx\right), \tag{9}$$

$$\frac{a^2}{12}\left(\frac{d\eta}{dx}\right)^2 = \frac{1}{4}v\phi_b^2(\eta^2-1)^2 - f\int_x^{\infty} \eta\zeta\frac{d\eta}{dx}dx. \tag{10}$$

Equation (10) is then multiplied by $2k_m^2/f$ and subtracted from Eq. (9).

Using $\int_x^{\infty}(d\zeta/dx)\eta^2 dx = -\eta^2\zeta - 2\int_x^{\infty}(d\eta/dx)\zeta\eta dx$ we get

$$\frac{1}{2}\left(\frac{d\zeta}{dx}\right)^2 - \frac{k_m^2a^2}{6f}\left(\frac{d\eta}{dx}\right)^2 = \kappa^2(\cosh\zeta - 1) + k_m^2(e^{\zeta}-1) - k_m^2\zeta\eta^2 - \frac{1}{2f}v\phi_b^2k_m^2(\eta^2-1)^2, \tag{11}$$

which can be interpreted as the local pressure balance equation. The first term on the left-hand side (LHS) of Eq. (11) is the electrostatic field pressure, and the second term is the pressure arising from chain elasticity. The first and second terms on the right-hand side (RHS) are the ideal gas pressure of the salt and counterions. The third term is the pressure due to the interaction between the electrostatic field and the monomer concentration, and the last term is the excluded-volume driven pressure.

For every segment where ζ is a monotonic function of x, a change of variables from x to ζ can be performed. Using $d\eta/dx=(d\eta/d\zeta)(d\zeta/dx)$ in Eq. (11) yields

$$\left(1 - \frac{k_m^2a^2}{3f}[\eta'(\zeta)]^2\right)\left(\frac{d\zeta}{dx}\right)^2 = 2\kappa^2(\cosh\zeta - 1) + 2k_m^2(e^{\zeta} - 1 - \zeta\eta^2) - \frac{1}{f}v\phi_b^2k_m^2(\eta^2-1)^2. \tag{12}$$

Below, for the strong repulsive case, we attempt to produce approximate solutions to Eqs. (11) and (12), and compare them to numerical calculations of Eqs. (3) and (4) (see also Ref. [10]).

Under the above assumptions, the excluded-volume term in Eq. (12) can be neglected, and $\exp(\zeta)$ and $\cosh(\zeta)$ can be expanded out to second order in ζ, yielding

$$\left(\frac{d\zeta}{dx}\right)^2 - \frac{k_m^2a^2}{3f}\left(\frac{d\eta}{d\zeta}\right)^2\left(\frac{d\zeta}{dx}\right)^2 = \kappa^2\zeta^2 + 2k_m^2\zeta(1-\eta^2) + k_m^2\zeta^2. \tag{13}$$

The first term on the RHS relates to the salt ions, the second to both the monomer and counterion concentrations, and the third term to the counterion concentration.

B. Scaling of potential and concentration profiles

Under the above assumptions, the dominant term in the RHS of Eq. (13) is the second one related to the monomer and counterion contributions. This term changes sign from negative to positive at $\eta \simeq 1$. For $\eta \to 0$ (close to the surface) the negative sign of the RHS implies that the second (negative) term of the LHS is dominant: $d\eta/d\zeta > \sqrt{3f/k_m^2a^2}$. Finally, it can be shown self-consistently (presented below) that the first term on the LHS is of order $|\zeta_s|^3$ while the correction terms on the RHS are of order $|\zeta_s|^2$. Hence close to the surface we neglect the first term in the LHS,

$$\frac{k_m^2a^2}{3f}\left(\frac{d\eta}{d\zeta}\right)^2\left(\frac{d\zeta}{dx}\right)^2 = 2k_m^2|\zeta|(1-\eta^2) - (k_m^2+\kappa^2)\zeta^2. \tag{14}$$

On the charged surface $\eta=0$ and $\zeta=-|\zeta_s|$. Using the mean-value theorem in the interval of interest $0 \leqslant \eta \leqslant 1$ we get $d\eta/d\zeta|_{y=y_s} \simeq 1/|\zeta_s|$. Substituting the scaling hypothesis $d\zeta/dx|_{x=0} \simeq |\zeta_s|/D$ in Eq. (14) evaluated at the surface yields an estimate for the layer thickness D:

$$D \simeq \frac{a}{\sqrt{6f|\zeta_s|}}\left(1 - \frac{\kappa^2+k_m^2}{2k_m^2}|\zeta_s|\right)^{-1/2} \simeq \frac{a}{\sqrt{6f|\zeta_s|}}\left(1 + \frac{1}{4}|\zeta_s| + \frac{c_{\mathrm{salt}}}{2f\phi_b^2}|\zeta_s|\right). \tag{15}$$

The first term of Eq. (15) retrieves the result given in Refs.

[7,10,12,14]. The other terms include corrections due to the ionic strength of the solution. As salt is added, the monomer-monomer electrostatic repulsion wins over the electrostatic attraction of the PE's to the surface, resulting in an increase in the adsorption length D, and at very high salt in depletion [10].

By changing x to the dimensionless length x/D, neglecting the excluded-volume term and inserting the potential scaling hypothesis in Eq. (4), the scaling form for the monomer concentration $\phi_b^2\eta^2$ can be derived. The scaling form of ζ [see assumption (iii) above] dictates a similar scaling form: $\eta=\phi(x)/\phi_b \simeq \sqrt{\phi_M^2/\phi_b^2}\, g(x/D)$, where ϕ_M^2 is the peak monomer concentration, and g is a scaling function normalized to one at the peak and satisfies $g(0)=0$.

To find ϕ_M^2, the peak concentration condition $d\eta/d\zeta=0$ can be inserted in Eq. (13), causing the second term on the LHS to vanish. Using the scaling for ζ and D of Eq. (15) yields

$$\phi_M^2 = \left(\phi_b^2 + \frac{3|\zeta_s|^2}{4\pi l_B a^2}\right)\left(1 - \frac{2c_{\text{salt}} + f\phi_b^2}{2f\phi_b^2}|\zeta_s|\right), \qquad (16)$$

where factors depending on the value of h, the scaling function for the potential, and its derivative evaluated at the peak position are omitted for clarity. The above equation is in agreement with previous results [7,10] calculated in the limit of no added salt and negligible effect of counterions. As the amount of salt increases, the monomer concentration characterized by ϕ_M^2 decreases, and for large enough amount of added salt, the peak monomer concentration decreases below its bulk value—a clear sign of depletion.

The amount of adsorbed monomers in the adsorption layer is now calculated as a function of ionic strength,

$$\Gamma \simeq \phi_{M,0}^2 D_0\left[1 - \frac{2c_{\text{salt}} + f\phi_b^2}{4f}|\zeta_s|\left(\frac{1}{\phi_b^2} + \frac{2}{\phi_{M,0}^2}\right)\right], \qquad (17)$$

where the added subscript zero denotes the known no-salt limits, $\phi_{M,0}^2 = 3|\zeta_s|^2/(4\pi l_B a^2)$ and $D_0 = a/\sqrt{6f|\zeta_s|}$, of the maximal monomer concentration ϕ_M^2 and adsorption length D, respectively [7,10]. For no added salt, the adsorbed amount scales like

$$\Gamma = \Gamma_0 \simeq \phi_{M,0}^2 D_0 \sim |\zeta_s|^{3/2} f^{-1/2} l_B^{-1} a^{-1}. \qquad (18)$$

When salt is added, the surface potential screening is obtained via the PE's and salt ions. In addition, the adsorbed amount Γ decreases as can be seen from the negative correction term in Eq. (17).

Using the above assumptions, the scaling of the induced surface charge is

$$|\sigma| = (4\pi l_B)^{-1}\left.\frac{d\zeta}{dx}\right|_{x=0} \sim \frac{|\zeta_s|}{4\pi l_B D} \sim \frac{|\zeta_s|^{3/2} f^{1/2}}{l_B a}. \qquad (19)$$

Comparing this scaling to Eq. (17), we see that the scaling of σ resembles that of the charge carried by the adsorbed amount $f\Gamma$. Subtracting the two equations shows that the overcharging $\Delta\sigma = f\Gamma - \sigma$ scales like σ as well.

The numerically calculated salt dependence of the adsorption length D is presented in Fig. 4(a). The location of the concentration peak, taken as D, is shown as a function of the bulk salt concentration c_{salt}. The length D is shown to increase with the addition of salt, in agreement with Eq. (15) and with experimental results [26,30]. The salt dependence of the overall adsorbed amount $\Gamma \equiv \phi_b^2 \int_0^\infty (\eta^2 - 1)dx$ is presented in Fig. 4(b). The adsorbed amount is shown to decrease steadily with the addition of salt, in agreement with Eqs. (17). The sharp drop in Γ is a sign of PE depletion in high salt conditions, and shows that the higher terms in the $\Gamma(c_{\text{salt}})$ expansion are negative as well.

We close this section by mentioning that a more elaborated treatment of the overcharging for strongly repulsive surfaces is presented in the Appendix. We find two different scaling regimes: one for electrostatically dominated overcharging and the second for the excluded volume dominated one. For the electrostatically dominated regime the overcharging follows the same scaling as the overall PE adsorption, $\Delta\sigma \sim \Gamma \sim f\sigma$. In the excluded volume dominated regime its scaling depends on the excluded volume parameter and yields $\Delta\sigma_0 \simeq f|\sigma|\sqrt{l_B a^2/(v^2\phi_b^2)}$. In both cases the magnitude of overcharging is very small as compared to the bare σ. This weak overcharging is not sufficient to explain PE multilayer formation for the repulsive surfaces considered in this section. Note that a very different situation exists when the surfaces are chemically attractive as discussed in Sec. III.

V. WEAK CHEMICALLY REPULSIVE SURFACES

In Sec. IV, we treated the strong chemically repelling surface, and concluded that the PE-surface electrostatic attraction is the sole drive for the adsorption. In this section, we relax the assumption of strong repulsive surfaces, while preserving the dominance of the electrostatic interactions.

The chemical interactions are added into our model via the amount of PE in direct contact with the adsorbing surface $\phi(x=0) \equiv \phi_s$ [or in the renormalized form $\eta(x=0)=\eta_s$]. We note that the case of weakly repulsive surfaces the slope of the monomer order parameter near the surface must be positive, $d\eta/dx|_{x=0} > 0$, as explained in Sec. II.

We begin by noting that the mean-field equations (3) and (4) are invariant to translations in the coordinate x. Namely, the equations are invariant under a translational transformation $x \to x+l$, as long as the boundary conditions are also transformed in the same manner, i.e., $\phi(l)=\phi_s$ and $\zeta(l) = -|\zeta_s|$. We note that this is a property of the planar geometry used in this case, and that for different geometries such as spherical or cylindrical this shift symmetry is no longer present.

Using the above symmetry, the adsorption profile characterized by $\phi(x)$, $\zeta(x)$, with boundary conditions $\phi(0)=\phi_s$, $\zeta(0) = -|\zeta_s|$, can be thought of as part of a larger profile, satisfying $\zeta(-l) \equiv -|\zeta_s^*|$ and $\phi(-l)=0$ at the $x=-l$ phantom surface. Such a profile, in turn, is exactly similar to the one discussed in the previous subsection, since the two systems are connected by the above mentioned translational transformation. Therefore finding the above ζ_s^* and l from the given

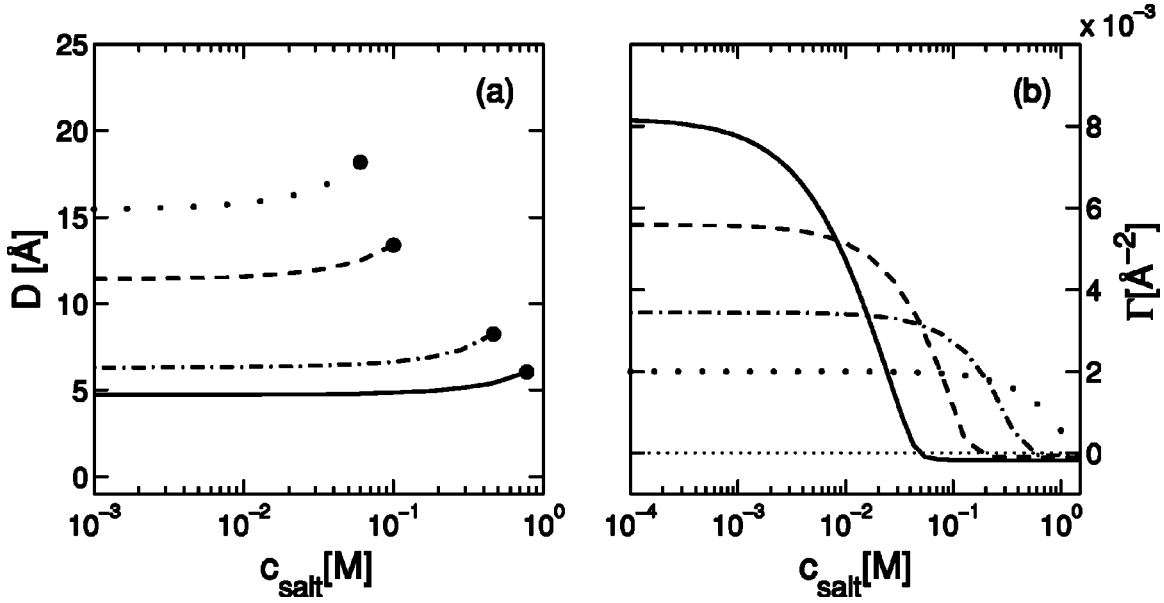

FIG. 4. (a) The width of the concentration profile D, taken as the peak location, is presented as a function of c_{salt}, the added-salt concentration. The dotted line corresponds to $f=0.1$, the dashed line to $f=0.18$, the dashed-dotted line to $f=0.56$, and the solid line to $f=1$. Other parameters used are $\varepsilon=80$, $T=300$ K, $|\zeta_s|=1$, $a=5$ Å, $\phi_b^2=10^{-6}$ Å^{-3}, $v=50$ Å^3. The length scale of the adsorption D is seen to increase with the addition of salt. For high enough added salt concentrations, the concentration peak vanishes altogether, indicating that the polymer is depleted from the surface. The adsorption-depletion crossover is denoted by a full circle. (b) The total adsorbed amount $\Gamma=\int_0^\infty dx(\phi^2-\phi_b^2)\sim c_m D$ is plotted against the amount of added salt. The solid line corresponds to $f=0.03$, the dashed line to $f=0.1$, the dash-dot to $f=0.31$ and the dotted line to $f=1$. The adsorbed amount decreases slowly with salt for low amounts of added salt. For high concentrations of added salt the adsorbed amount decreases sharply to negative values, signaling an adsorption-depletion transition. Other parameters used are the same as in (a) (reproduced from Ref. [10]).

ϕ_s, $|\zeta_s|$ then enables the derivation of the adsorption characteristics in the same manner as discussed in Sec. IV.

This strategy is demonstrated in Fig. 5. In Fig. 5(a) the monomer concentration profiles are presented as a function of the distance from the surface x for several surface parameters $0<\phi_s<16.2\phi_b$ and $0<|\zeta_s|<1.0$. The profiles were obtained by solving Eqs. (3) and (4) numerically using the boundary conditions $\eta(0)=\phi_s/\phi_b$, $\zeta(0)=-|\zeta_s|$ close to the surface and $\zeta(x\to\infty)=0$, $\eta(x\to\infty)=1$ at infinity. In Fig. 5(b) the same profiles are shown, with a translation in the surface position. As can be seen in Fig. 5(b), all three profiles collapse on exactly the same profile, showing that all three profiles have the same concentration and length scales despite the difference in $|\zeta_s|$ and η_s. These scales can be calculated by using Eqs. (15) and (16), as discussed in the previous subsection.

Using the scaling relations Eqs. (15) and (16), the above symmetry yields the following connections between $|\zeta_s^*|$, l and the surface boundary conditions $|\zeta_s|$ and ϕ_s:

$$\phi_s=\phi_M^* g\left(\frac{l}{D^*}\right), \tag{20}$$

$$\zeta_s=|\zeta_s^*|h\left(\frac{l}{D^*}\right), \tag{21}$$

where D^*, ϕ_M^* are the same as Eqs. (15) and (16) when we change $|\zeta_s|\to|\zeta_s^*|$. Manipulation of Eq. (21) then yields

$$|\zeta_s^*|=\frac{\zeta_s}{h(l/D^*)}=\frac{\zeta_s}{h(g^{-1}(\phi_s/\phi_M^*))}. \tag{22}$$

Equation (22) can be solved iteratively for $|\zeta_s^*|$ potential as a function of the surface and bulk solution parameters. Insertion of the result into Eq. (21) then gives l/D^*.

It is important to note that the inversion of Eq. (21) is only possible in the region where ϕ and x are monotonic, i.e., when the surface monomer concentration is lower than the maximal monomer concentration on the profile $\phi_s^2<\phi_{\mathrm{max}}^2$. This condition can also be expressed by the condition $d\eta/dx|_{x=0}>0$, showing that the chemical interactions between the surface and the PE chains must still be repulsive for the shift strategy to be employed.

We now proceed to solve Eq. (22) for low values of ϕ_s/ϕ_M. Using the boundary conditions and Eqs. (3) and (4) the characteristic functions $h(x')$, $g(x')$ can be expanded in powers of x' to yield $g(x')=a_0x'+b_0x'^3+\cdots$ and $h(x')=-1+a_1x'+b_1x'^2+\cdots$. Inserting these expansions into Eq. (22) and solving to second order in ϕ_s yields

$$|\zeta_s^*|=|\zeta_s|\left[1+\frac{a_1}{a_0}\frac{\phi_s}{\phi_M}\right]+\cdots. \tag{23}$$

Note that ϕ_M^2 is now no longer the actual maximal monomer concentration, but is defined in Eq. (16) as the characteristic for the monomer concentration, where the real surface electrostatic potential $|\zeta_s|$ is used rather than the phantom surface potential.

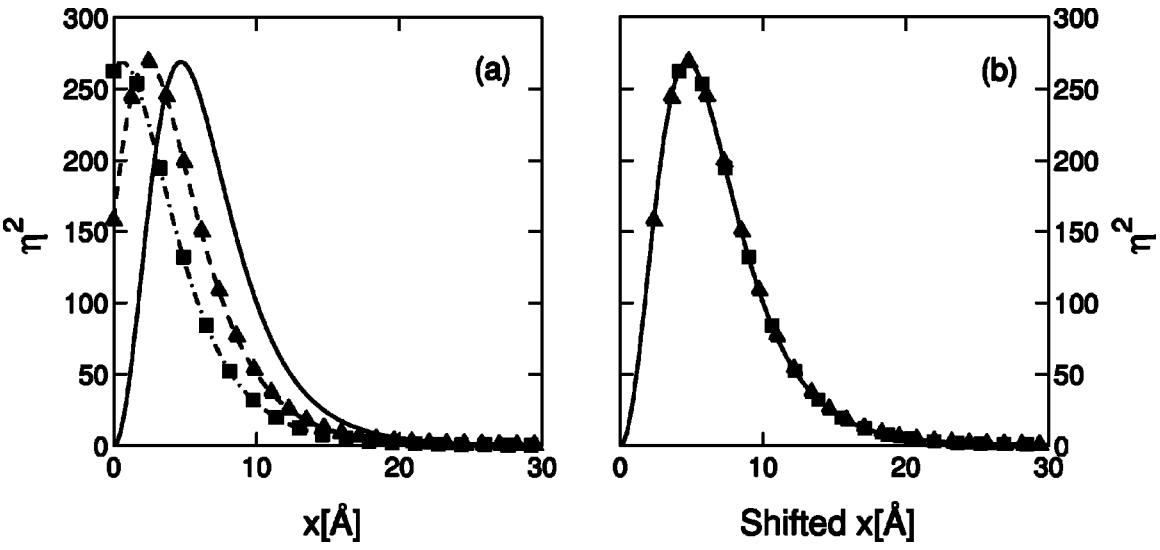

FIG. 5. (a) The numerically calculated monomer concentration $\eta^2(x)$ is plotted as a function of the distance from the charged surface x, for several values of $|\zeta_s|$ and $\eta_s \equiv \phi_s/\phi_b$. The solid line corresponds to $\eta_s=0$ and $|\zeta_s|=1.0$, the dashed line with triangle markers to $\eta_s=12.55$ and $|\zeta_s|=0.6$, and the dashed-dotted line with square markers to $\eta_s=16.2$ and $|\zeta_s|=0.34$. All profiles share $c_{\text{salt}}=0.01M$, $f=1$, $a=5$ Å, $v=10$ Å^3, $\phi_b^2=10^{-6}$ Å^{-3}, $\varepsilon=80$, and $T=300$ K. All profiles are found to have the same height in the peak monomer concentration, despite the difference in the boundary conditions. (b) The same profiles as in part (a), after a shift in the $x=0$ position is used. The solid line is not shifted, the dashed line with triangular markers is shifted by $\Delta x=2.35$ Å, and the dashed-dotted line with square markers is shifted by $\Delta x=4.12$ Å. All three profiles, show a data collapse on the solid line profile, corresponding to $|\zeta_s^*|=1.0$.

We can now turn to calculate the overall adsorption. Returning to the initial assumption that the monomer concentration profile is a part of a larger profile starting at $x=-l$, the adsorbed amount can be taken as the total adsorbed amount from $x=-l$ to infinity, minus the amount adsorbed from $x=-l$ to the actual surface at $x=0$:

$$\Gamma = \int_0^\infty dx(\phi^2 - \phi_b^2) = \int_{-l}^\infty dx(\phi^2 - \phi_b^2) - \int_{-l}^0 dx(\phi^2 - \phi_b^2). \tag{24}$$

The first integral in the RHS of Eq. (24) is the overall adsorption of PE to the phantom surface at $x=-l$, while the second integral is the PE adsorbed amount between this phantom surface and the real surface at $x=0$. Using the expansion of $g(x)$ and Eq. (20), we can see that the second integral is of third order in ϕ_s/ϕ_M, and can be neglected for low enough ϕ_s/ϕ_M. Using Eqs. (17) and (20), Eq. (24) can be evaluated as

$$\Gamma \simeq \frac{\sqrt{3}|\zeta_s|^{3/2}}{4\pi\sqrt{2}l_B a f^{1/2}}\left[1 - \frac{2c_{\text{salt}} + f\phi_b^2}{4f\phi_b^2}|\zeta_s| + \frac{3a_1\phi_s}{2a_0\phi_{M,0}} \times\left(1 + \frac{2c_{\text{salt}} + f\phi_b^2}{12f\phi_b^2}|\zeta_s|\right)\right]. \tag{25}$$

As expected, the adsorbed amount increases with ϕ_s. However, the salt dependence of the surface is very different from the strongly repulsive surface case. For low amounts of added salt and high enough ϕ_s, the term combining the small ions and ϕ_s is stronger than the salt term, and the adsorbed amount *increases* with salt. When ϕ_s is low, the addition of salt causes the adsorbed amount to decrease, similar to the strongly repulsive surface case. In both cases, when the amount of salt increases to a high enough value, higher order terms become dominant, and the adsorbed amount *decreases*, similar to the infinitely repulsive case in Fig. 4(b).

The salt dependence of the adsorbed amount Γ is shown for several ϕ_s values in Fig. 6(a). The adsorbed amount is shown to always increase with the amount of monomers attached to the surface ϕ_s^2. For low ϕ_s values, the adsorbed amount decreases with salt, as expected from Eq. (25) and in agreement with Fig. 4(b). For higher ϕ_s values, the adsorbed amount is seen to increase for low bulk concentrations of salt and then decrease strongly. In Fig. 6(b) the relative overcharging is plotted for the same ϕ_s values, showing that the relative overcharging is still a very small effect, even for weakly repulsive surfaces. This shows that the attractive chemical interactions between the surface and the PE chains are indeed crucial for the multilayer formation, and not the electrostatic interactions alone.

VI. DISCUSSION AND CONCLUSIONS

We have presented analytical and numerical calculations of the mean-field equations describing adsorption of polyelectrolytes onto charged surfaces. Three surface situations are discussed: chemically attractive surfaces, and strong and weak chemical repulsive ones.

The strongest adsorption phenomenon is seen from numerical solution of the mean-field equations for chemically attractive surfaces. This manifests itself in a large overcharging of about 40–55 % of the bare surface charge for high salt conditions. On the other hand, we did not find a full charge inversion as was predicted earlier in Ref. [6]. This means that any model [27,28] which tries to explain multilayer forma-

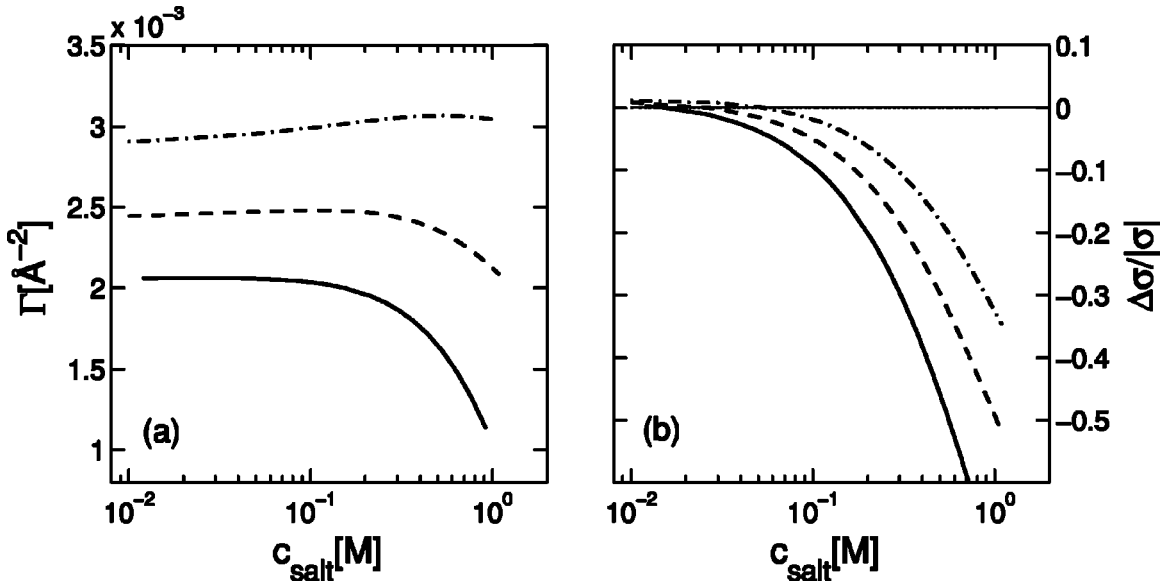

FIG. 6. (a) Numerically calculated adsorbed amount of monomers Γ is plotted against the added salt concentration c_{salt} for several values of $\eta_s=\phi_s/\phi_b$, for the case of weak chemically repulsive surfaces. The solid line corresponds to $\eta_s=5$, the dashed line corresponds to $\eta_s=50$, and the dashed-dotted line to $\eta_s=100$. All profiles share $|\zeta_s|=1.0$, $f=1.0$, $a=5$ Å, $v=10$ Å^3, $\phi_b^2=10^{-8}$ Å^{-3}, $\varepsilon=80$, and $T=300$ K. The adsorbed amount is seen to increase with η_s for all values of c_{salt}. For low amounts of added salt, the adsorbed amount is seen to increase with salt, in contrast to the $\eta_s=0$ case (strong repulsive surface) in Fig. 4(b), while for high amounts of added salt the adsorbed amount decreases, in agreement with Fig. 4(b). (b) The relative overcharging $\Delta\sigma/|\sigma|$ is plotted against the amount of added salt for the same parameters as in part (a). Despite the increase in the adsorbed amount, the relative overcharging remains a very small effect. At high salt concentration, the relative overcharging becomes negative—signaling an *undercompensation* of the surface charge.

tion at equilibrium needs to rely on nonelectrostatic complexation between the cationic and anionic polymer chains, beside the electrostatic interactions. So far no simple scaling forms are obtained for the PE adsorbed amount in this case. However, the adsorbed amount (and the overcharging) are shown to increase with the salt amount c_{salt}, and to decrease with f, the charge fraction on the PE chain as well as with d, which is inversely proportional to the chemical interaction of the surface.

For the case of strong chemical repulsion between the surface and the PE chains, we find a difference in the effect of salt addition on the width of the adsorbed layer D and on the adsorbed PE amount Γ (Fig. 4). The width of the PE adsorbed layer increases with the addition of salt, while the overall adsorbed PE amount *decreases* with the addition of salt. This difference results from a strong decrease in the monomer concentration close to the surface upon the addition of salt. This difference between Γ and D is in agreement with experimental results of Shubin *et al.* [30], where silica surfaces were used to adsorb cationic polyacrylamide (CPAM). When salt is further added to the solution, the PE's stop overcompensating the charged surface, and we are in an undercompensation regime of adsorption. Previous studies [10] showed that for even higher amounts of salt, scaling as $c_{\mathrm{salt}}\sim f|\phi_s|$, the PE's deplete from the charged surface. For such surfaces, the overcharging in most cases is found to scale like the induced surface charge density σ. For weakly charged PE's the overcharging depends on the excluded-volume parameter and bulk monomer concentration, and scales as $\sim f\sigma$. Very weakly charged PE's are shown to adsorb to the charged surface, but do not overcharge it. Our scaling results are in agreement with numerical calculations of the mean-field equations. For all PE charges, the overcharging of the PE with respect to a repelling surface is found to be very small, of the order of 1% of the bare surface charge. This naturally leads to the conclusion that the overcharging relies heavily on the chemical interactions between the surface and the PE chains. It is of much smaller importance for this type of repulsive surfaces than for attractive ones considered above.

For weakly repulsive surfaces, we find that the adsorbed amount increases with the addition of salt for low salt amounts, and decreases for high amounts of added salt. This is a natural interpolation between the attractive and repulsive surface limits. Moreover, the overcharging of the surface charge remains low, and for high amounts of added salt the PE again undercompensates the surface charges.

Our results can serve as a starting point for a more quantitative analysis of the overcharging phenomena, and provide for better understanding of multilayer formation.

ACKNOWLEDGMENTS

We thank I. Borukhov, Y. Burak, M. Castelnovo, J.-F. Joanny, and E. Katzav for useful discussions and comments. In particular, we are indebted to Qiang (David) Wang for his critical comments on a previous version of this manuscript. Support from the Israel Science Foundation (ISF) under Grant No. 210/01 and the U.S.-Israel Binational Foundation (BSF) under Grant No. 287/02 is gratefully acknowledged.

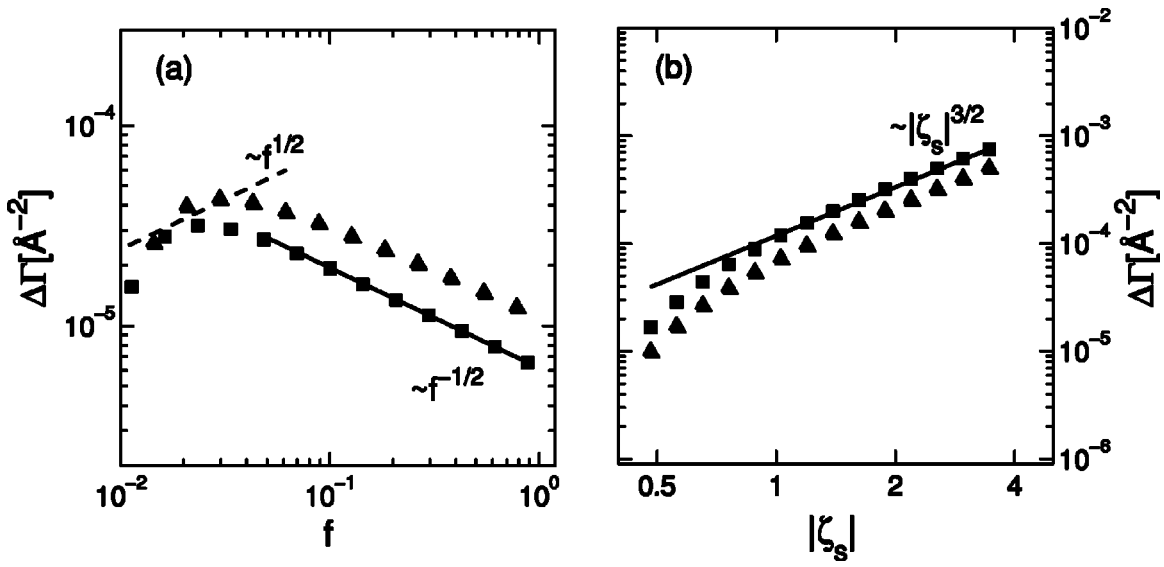

FIG. 7. (a) Numerically calculated excess adsorption $\Delta\Gamma$, defined as the PE adsorbed amount from the potential peak to infinity, is plotted against f. The squares correspond to $|\zeta_s|=0.5$, and the triangles to $|\zeta_s|=0.6$. Both profiles share $\phi_b^2=10^{-6}$ Å^{-3}, $v=10^2$Å^3, $a=5$ Å, $c_{\text{salt}}=0.1$ mM, $T=300$ K, and $\varepsilon=80$. The two profiles can be fitted in the low f region by $\Delta\Gamma\sim f^{1/2}$ (dashed line), followed by a high f region where $\Delta\Gamma\sim f^{-1/2}$ (solid line). These scaling results are in agreement with Eqs. (A3) and (A6). (b) $\Delta\Gamma$ is plotted against the surface potential $|\zeta_s|$. The squares correspond to $f=0.1$, and the triangles to $f=0.3$. All other parameters are the same as in (a). The two profiles show a scaling of $\Delta\Gamma\sim|\zeta_s|^{3/2}$, fitted by a solid line, in agreement with Eqs. (A3) and (A6). The constant prefactors in the fitting lines are obtained by imposing the condition that the fitting line passes through the last numerical data point in the respective regime.

APPENDIX: SCALING OF THE OVERCHARGING LAYER IN CHEMICALLY REPULSIVE SURFACES

In order to derive scaling estimates for the PE adsorption regime, the adsorbed PE layer is divided into two sublayers around the potential peak point $x\equiv x_c$. The compensation layer is defined as $x<x_c$, and consists of PE's attracted to the surface mainly by electrostatics. In contrast, in the overcharging layer ($x>x_c$) the PE chains are electrostatically repelled from the surface, but remain in the surface vicinity solely because of their chain connectivity. For low enough salt concentrations, the amount of charge carried by the PE's in the adsorbed layer is much larger than that carried by the small ions. In this case, the overcharging can be taken as

$$\Delta\sigma\equiv-|\sigma|+f\phi_b^2\int_0^\infty dx(\eta^2-1)\simeq f\phi_b^2\int_{x_c}^\infty dx(\eta^2-1), \tag{A1}$$

where the first integral is the same as Eq. (7), with σ being the *induced* surface charge on the adsorbing surface. The second integral in the above equation is taken from $x=x_c$ to infinity, and describes the PE adsorption in the region where the electrostatic interaction between the PE and the surface is repulsive. The integral from $x=0$ to x_c balances the surface charge almost entirely for low amounts of added salt, using the fact that $d\zeta/dx|_{x_c}=0$ (Gauss law).

In order to find the amount of polymers in the overcharging layer, we begin by examining Eq. (11) at the potential peak, $x=x_c$, where the first term on the LHS vanishes. Expanding the RHS to second order in ζ without neglecting the excluded-volume term yields

$$\left.\frac{a^2}{6}\left(\frac{d\eta}{dx}\right)^2\right|_{x=x_c}=f\zeta_c(\eta_c^2-1)+\frac{1}{2}v\phi_b^2(\eta_c^2-1)^2-\frac{f}{2}\left(\frac{\kappa^2}{k_m^2}+1\right)\zeta_c^2, \tag{A2}$$

where the values at the peak are denoted by $\zeta_c\equiv\zeta(x_c)$ and $\eta_c\equiv\eta(x_c)$. As shown below, η_c decreases with addition of salt. Therefore, for a large amount of added salt, the LHS of Eq. (A2) becomes negative (this is true to all orders of ζ_c and not only to order ζ_c^2 as shown here), while the RHS is always positive, meaning that there is no peak in the rescaled potential ζ. This demonstrates that surface charge overcharging can only occur in low enough salt conditions.

In the overcharging layer, the previous assumptions made in Sec. III A about the dominance of the electrostatic interactions are not necessarily true. Consequently, the decay of the PE concentration in this region can be governed by either one of two interactions: the electrostatic or the *excluded-volume* repulsion between the monomers. We consider them as two limits for overcharging. (i) An electrostatically dominated regime, $v\phi_b^2(\eta_c^2-1)\ll f\zeta_c$, where the excluded-volume term is neglected in Eq. (A2). (ii) The excluded-volume dominated regime, $v\phi_b^2(\eta_c^2-1)\gg f\zeta_c$. Here, the electrostatic interaction between monomers in Eq. (A2) is neglected. In both regimes the value of $d\eta/dx$ at the peak position is estimated from the scaling of the compensation layer to be $d\eta/dx|_{x=x_c}\simeq\phi_M/(\phi_b D)$.

1. Strongly charged regime: $v\phi_b^2(\eta_c^2-1)\ll f\zeta_c$

The validity criterion of this regime is similar to the assumptions presented in Sec. IV A, showing that the over-

charging layer ($x>x_c$) can be thought of as an extension of the compensation layer ($0<x<x_c$). Instead of rederiving $\Delta\sigma$ from Eq. (A2), we can use Eq. (14) and the expressions for D and ϕ_M^2 from Eqs. (15) and (16), which yield $\zeta_c \sim |\zeta_s|$ and $\eta_c^2 \sim \phi_M^2/\phi_b^2$. The resulting overcharging scales like the bare surface charge:

$$\Delta\sigma \sim f\Gamma_D \sim f(\phi_M^2 - \phi_b^2)D \sim |\sigma|. \tag{A3}$$

Note that the effect of added salt in this regime is similar to the one described in Eq. (17). Namely, the added salt lowers the surface charge overcharging, in agreement with experimental [30] and numerical [10] results.

2. Intermediate charged regime: $v\phi_b^2(\eta_c^2-1) \gg f\zeta_c$

In this regime, the excluded-volume interactions dominate the decay of the PE concentration. Using the regime validity condition and neglecting the first term on the RHS of Eq. (A2) yields an expression for the monomer concentration at x_c:

$$\eta_c^2 = 1 + \sqrt{\frac{a^2}{3v\phi_b^2}\left(\frac{d\eta}{dx}\right)^2\Bigg|_{x=x_c} + \frac{\kappa^2+k_m^2}{k_m^2 v\phi_b^2} f\zeta_c^2}. \tag{A4}$$

Noting that the $d\eta/dx$ is continuous at $x=x_c$, we use the compensation layer scaling estimates to find $d\eta/dx|_{x=x_c} \simeq \phi_M/(\phi_b D)$. Substituting the latter into Eq. (A4) and expanding to first order in both the ionic strength $2c_{\rm salt}+f\phi_b^2 = (\kappa^2+k_m^2)/4\pi l_B$ and the ratio of the bulk and peak monomer concentrations $\phi_b^2/\phi_M^2 \simeq l_B a^2 \phi_b^2/|\zeta_s|^2$ yields

$$\eta_c^2 \simeq 1 + \sqrt{\frac{3}{2\pi}}\frac{|\zeta_s|^{3/2} f^{1/2}}{\sqrt{l_B a^2 v}\,\phi_b^2}\left[1 - \frac{2c_{\rm salt}+f\phi_b^2}{2f\phi_b^2}|\zeta_s| + \frac{2\pi l_B a^2 \phi_b^2}{3|\zeta_s|^2}\right], \tag{A5}$$

where Eqs. (15) and (16) are used for D and ϕ_M^2, respectively.

The overcharging is calculated from Eq. (7) where the characteristic length scale entering the integral is the Edwards length, $\xi_e = a/\sqrt{3v\phi_b^2}$, depending only on the excluded-volume interactions and not on the salt. The overcharging $\Delta\sigma \simeq f\phi_b^2(\eta_c^2-1)\xi_e$ is

$$\Delta\sigma \simeq \frac{|\zeta_s|^{3/2} f^{3/2}}{\sqrt{2\pi l_B \phi_b^2 v}}\left[1 - \frac{2c_{\rm salt}+f\phi_b^2}{2f\phi_b^2}|\zeta_s| + \frac{2\pi l_B a^2 \phi_b^2}{3|\zeta_s|^2}\right]. \tag{A6}$$

In the limit of no ionic strength ($c_{\rm salt}=0$ and negligible counterion contribution), the overcharging from Eq. (A6) scales like $\Delta\sigma_0 \simeq f|\sigma|\sqrt{l_B a^2/(v^2\phi_b^2)}$. Addition of salt results in a decrease of overcharging, similar to what was shown in the previous subsection for the strongly charged regime.

By comparing the corresponding expressions for $f\zeta_c$ and $v\phi_b^2(\eta_c^2-1)$ in both regimes, we conclude that the boundary between the strongly charged and intermediate regimes occurs at $f \simeq 3v|\zeta_s|/(2\pi l_B a^2)$ (see also Ref. [7]). This serves as a self-consistency test.

We define the adsorption excess $\Delta\Gamma$ by integrating numerically the adsorbed amount from x_c to ∞. Note that in the low salt limit, $f\Delta\Gamma \simeq \Delta\sigma$ can be thought of as the overcharging parameter used earlier. It is then possible to make a direct comparison with the two limits discussed above. The adsorption excess as a function of f is presented in Fig. 7(a). For small f values, $\Delta\Gamma$ scales like $f^{1/2}$, in agreement with Eq. (A6), while for larger values of f the excess adsorption $\Delta\Gamma$ scales like $f^{-1/2}$, in agreement with Eqs. (18) and (A3). These two limiting scaling behaviors are shown in Fig. 7(a). In Fig. 7(b), $\Delta\Gamma$ is presented as a function of $|\zeta_s|$. The scaling $\Delta\Gamma \sim |\zeta_s|^{3/2}$, also shown in the figure, is in agreement with Eqs. (18), (A3), and (A6). We note, by comparing Fig. 4(b) to Fig. 7, that the overcompensating PE's are of the order of less than 1% of the total adsorbed amount, showing that the mean-field overcharging of repulsive surfaces is an extremely small effect.

3. Undercompensation threshold

So far we presented the case where the PE layer is overcompensating the surface charge, and discussed it in two limits of strong and intermediate charged PE's. In some range of system parameters the PE charges do not overcompensate the surface ones. The threshold for having this *undercompensation* is briefly discussed here.

Re-examining the validity of Eq. (A2), it can be seen that for high enough salt the third term on the right dominates the largest of the first two terms when

$$c_{\rm salt} + \frac{1}{2}f\phi_b^2 > \frac{f|\zeta_s|}{l_B a^2} \tag{A7}$$

up to some numerical pre-factors. Note that the same inequality is valid in both limits of strong and intermediate regimes, as long as we are in high salt conditions. It should be noted that a similar scaling rule was found in Refs. [1,2,10,14] for the adsorption-depletion crossover. Numerical results show that the overcharging-undercompensation transitions indeed have the same scaling, but differ in the constant multiplying the scaling result.

[1] F.W. Wiegel, J. Phys. A **10**, 299 (1977).
[2] M. Muthukumar, J. Chem. Phys. **86**, 7230 (1987).
[3] X. Chatellier and J.F. Joanny, J. Phys. II **6**, 1669 (1996).
[4] R. Varoqui, A. Johner, and A. Elaissari, J. Chem. Phys. **94**, 6873 (1991).
[5] R. Varoqui, J. Phys. II **3**, 1097 (1993).
[6] J.F. Joanny, Eur. Phys. J. B **9**, 117 (1999).
[7] I. Borukhov, D. Andelman, and H. Orland, Macromolecules **31**, 1665 (1998); Europhys. Lett. **32**, 499 (1995).
[8] I. Borukhov, D. Andelman, and H. Orland, Eur. Phys. J. B **5**,

869 (1998).
[9] I. Borukhov, D. Andelman, and H. Orland, J. Phys. Chem. B **103**, 5042 (1999).
[10] A. Shafir, D. Andelman, and R.R. Netz, J. Chem. Phys. **119**, 2355 (2003).
[11] M. Manghi and M. Aubouy, e-print cond-mat/0202045.
[12] O.V. Borisov, E.B. Zhulina, and T.M. Birshtein, J. Phys. II **4**, 913 (1994).
[13] R.R. Netz and J.F. Joanny, Macromolecules **32**, 9013 (1999).
[14] A.V. Dobrynin, A. Deshkovski, and M. Rubinstein, Macromolecules **34**, 3421 (2001).
[15] R.R. Netz and D. Andelman, in *Encyclopedia of Electrochemistry*, edited by M. Urbakh and E. Giladi (Wiley-VCH, Weinheim, 2002), Vol. I.
[16] R.R. Netz and D. Andelman, Phys. Rep. **380**, 1 (2003).
[17] H.A. van der Schee and J. Lyklema, J. Phys. Chem. **88**, 6661 (1984).
[18] O.A. Evers, G.J. Fleer, J.M.H.M. Scheutjens, and J. Lyklema, J. Colloid Interface Sci. **111**, 446 (1986).
[19] M.R. Böhmer, O.A. Evers, and J.M.H.M. Scheutjens, Macromolecules **23**, 2288 (1990).
[20] H.G.M. van de Steeg, M.A. Cohen Stuart, A. de Keizer, and B.H. Bijsterbosch, Langmuir **8**, 2538 (1992).
[21] V. Yamakov, A. Milchev, O. Borisov, and B. Dünweg, J. Phys.: Condens. Matter **11**, 9907 (1999).
[22] M. Ellis, C.Y. Kong, M. Muthukumar, J. Chem. Phys. **112**, 8723 (2000).
[23] J. McNamara, C.Y. Kong, and M. Muthukumar, J. Chem. Phys. **117**, 5354 (2002).
[24] Yu. Lvov, G. Decher, H. Haas, H. Möhwald, and A. Kalachev, Physica B **198**, 89 (1994).
[25] G. Decher, Science **277**, 1232 (1997).
[26] U. Voigt, V. Khrenov, K. Tauer, M. Halm, W. Jaeger, and R. von Klitzing, J. Phys.: Condens. Matter **15**, S213 (2003).
[27] M. Castelnovo and J.F. Joanny, Langmuir **16**, 7524 (2000).
[28] M. Castelnovo and J.F. Joanny, Eur. Phys. J. E **6**, 377 (2001).
[29] P.G. de Gennes, Macromolecules **14**, 1637 (1981).
[30] V. Shubin and P. Linse, J. Phys. Chem. **99**, 1285 (1995).